

Piezoelectric Strain Sensor through Reverse Replication based on Two-photon Polymerization

Rishikesh Srinivasaraghavan Govindarajan^a, Taylor Stark^a, Stanislav Sikulskyi^a, Foram Madiyar^b,
Daewon Kim^{*a}

^aDept. of Aerospace Engineering; ^bDept. of Physical Science;
Embry-Riddle Aeronautical University, 1 Aerospace Blvd., Daytona Beach, FL, USA 32114

ABSTRACT

High-performance piezoelectric sensors based on the polymer-based composite with inorganic filler have shown great potential as they offer unique properties and design flexibility. This paper aims to investigate the impact of nanoparticles on the piezoelectric property enhancement of the developed composite. The two-photon polymerization method using IP-Q resin is employed to fabricate the Interdigital transducer (IDT) design master mold for the piezoelectric substrate. Polyvinylidene trifluoroethylene (PVDF-TrFE)/barium titanate (BaTiO₃) substrate is fabricated by reverse mold replication. IDT channels are filled with conductive material through the screen-printing technique. The crystalline phase characteristics and surface morphology of fabricated substrate are examined using Fourier transform infrared spectroscopy and scanning electron microscope. Strain detection of the developed sensor is evaluated by determining the change in scattering parameters using a network analyzer.

Keywords: flexible sensor, nanocomposite, two-photon polymerization, strain detection

1. INTRODUCTION

Compelling benefits, such as expense adequacy, effectively processable and mechanically adaptable with properties that can be tailored, have impelled the development of a flexible piezoelectric sensor for structural health monitoring applications in the aerospace and bio-medical fields ^{1, 2}. The necessity of monitoring physical deformations occurring in aerospace structures during flight, demands an unobtrusive and intelligent sensing device to ensure safety. Acoustic wave-based piezoelectric composite sensors, being highly sensitive, self-powered, and suitable for a higher frequency range with stability, have attracted great interest in measuring mechanical strains. These wave-based piezoelectric sensors generally consist of a piezoelectric substrate, interdigital transducers (IDTs) placed at a certain distance named delay line where the generated wave propagates.

The piezoelectric response of the composite sensor can be dictated by several factors, such as the polymer-filler distribution, the weight fraction of added fillers, and poling conditions. A 0-3 composite with ceramic particles surrounded three-dimensionally by polymer matrix is the commonly used type for large-scale production due to its ease of fabrication ^{3, 4}. A composite substrate comprising organic ferroelectric polymer incorporated with inorganic fillers offers unique characteristics such as flexibility along with ferroelectric properties. Polyvinylidene fluoride (PVDF) and its copolymer polyvinylidene trifluoroethylene (PVDF-TrFE) are widely used as a polymer matrix in sensor applications due to their mechanical property compliance, lightweight nature, and easy processing. TrFE inclusion into PVDF forms a non-volatile, less dense copolymer, favoring a direct formation of ferroelectric β phase, which simplifies the fabrication process by eliminating the complicated post-processing procedures, such as stretching and crystallization under higher pressure ⁵. However, their piezoelectric properties, such as dielectric constant and piezoelectric coefficients, are low compared to ceramic materials. Functional inorganic ceramic fillers such as lead zirconate titanate (PZT) and barium titanate (BaTiO₃, BT) are commonly used active components due to their high piezoelectric strain coefficient and dielectric constant values ^{6, 7}. Perovskite BT is a favorable candidate over PZT due to its lead-free, low-cost environmental, and health-friendly characteristics ^{8, 9}.

Furthermore, the IDT electrode initiates the generation of waves that are analyzed further with the sensed frequency response. Rapid prototyping of the electrode pattern evades the design complexity and limitations of conventional lithographic techniques. Compared to the IDT electrode deposited on the surface, studies demonstrate enhancement of electrocoupling coefficient (k^2) by burying the electrode in the piezoelectric layer¹⁰. In this work, electrodes are embedded in the substrate, protecting the IDT from external damage with effective wave generation. The piezoelectric sensors are commonly manufactured using hot-press, melt extrusion, and conventional lithographic techniques^{4, 11}. Due to the design limitations, additive manufacturing is suitable to develop sensors with higher reliability.

Additive manufacturing (AM) has been an interest for the public and private sectors since it has the advantages of printing complex geometries with minimized material waste and reducing manufacturing costs¹²⁻¹⁴. Most additive manufacturing techniques such as fused deposition modeling and powder bed fusion produce large macro parts, but the method of two-photon polymerization (2PP) allows for extremely high resolution along with micro to nanometer features¹². 2PP helps fabricate nearly any small 3D structure using direct laser writing (DLW) and allows design changes to be made and tested promptly^{12, 15}. This paper presents a novel reverse replication technique of piezoelectric substrate, as shown in Figure 1, which exhibits enhanced piezoelectric properties with embedded electrodes capable of detecting mechanical strains.

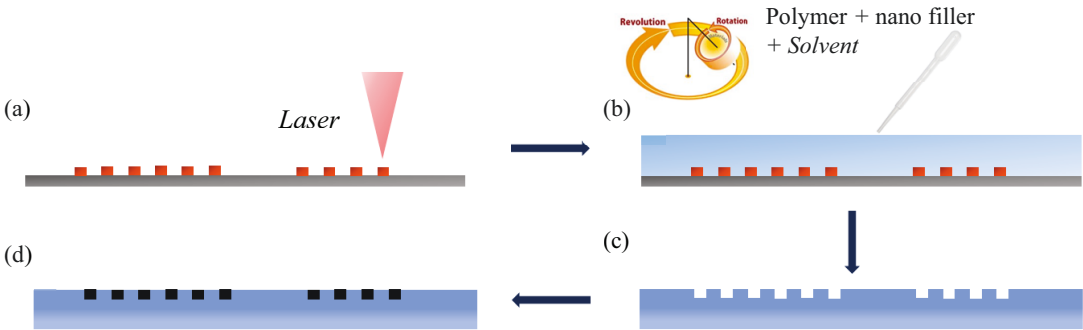


Figure 1. Reverse replication process of a piezoelectric substrate with embedded electrodes. (a) 2PP printing of master mold, (b) positive mold made of polymer-nanofiller composite, (c) positive mold after peeling off, and (d) conductive electrode deposition.

2. REVERSE REPLICATION FABRICATION OF NANOCOMPOSITE SUBSTRATE

2.1 Master mold using 2PP

A master mold with IDT design is developed on a 2-inch silicon wafer to replicate the piezoelectric sensor with empty electrode channels. The IDT master mold made of high viscous negative photoresist (IP-Q, Nanoscribe, Karlsruhe, Germany) is printed using a 2PP printer (Photonic Professional GT2, Nanoscribe GmbH, Karlsruhe, Germany) equipped with a 780 nm femtosecond laser. IP-Q resin and the 0.3 numerical aperture lens are utilized for increasing the voxel size with quicker modeling of the mesostructured IDT master mold.

Table 1. IDT master mold dimensions used in 2PP printing

Parameters	Dimension
Finger width (Free space width) [μm]	125
Metallized ratio (η)	0.5
Wavelength (λ) [μm]	500
No. of input (output) finger pair	3 (2)
Acoustic aperture [μm]	850
Depth of IDTs [μm]	300
Delay line distance [μm]	1000
Bus bar width [μm]	150

After cleaning the silicon wafer using acetone and isopropanol, the wafer is activated with an oxygen plasma etch PE-50HF system (Plasma Etch, Caron City, USA) at a pressure of 149.8 mTorr, a flow rate of 20 cc/min, and a radio frequency (RF) power of 20 W for 40 seconds. The printer parameters used are 4 μm slicing distance, 1 μm hatching distance, 100 mm/scan, and 90% laser power. The printed master mold is developed for 20 min in propylene glycol monomethyl ether acetate (PGMEA) (Merck kGaA, Darmstadt, Germany), developed for 5 min in isopropanol, and dry-blown with compressed air. Master mold dimensions printed using a 2PP printer are mentioned in Table 1.

2.2 Piezoelectric substrate development

To develop a flexible piezoelectric composite, PVDF-TrFE incorporated with BT particles is fabricated through a novel replication process. Primary materials selected for the piezoelectric composites are listed below:

- PVDF-TrFE powder 80/20 mol (PolyK, State College, PA, USA), a density of 1.88 g/mL and Curie temperature of 135 $^{\circ}\text{C}$.
- BaTiO₃ (BT) 99.5% purity (TPL Inc., Albuquerque, NM, USA), near-spherical particles with an average diameter of 420 nm, the specific surface area of 4 m²/g, and density of 6 g/cm³.
- DMSO (Sigma-Aldrich, St. Louis, MO, USA), Mw ~78.13 g/mol.

PVDF-TrFE polymer is dissolved in polar solvent dimethyl sulfoxide (DMSO) due to the polymer insolubility in water using a planetary THINKY mixer (Laguna Hills, CA, USA) for 12 min at 2000 rpm. The dissolved base polymer PVDF-TrFE is then mixed with different wt. % proportions (40% and 60 %) of the BT ceramic particles. Particles are well mixed with the base polymer in both rotational and revolution axed motion without bubbles due to the deaeration capability of the mixing technique used. The mixture is then poured into a custom-made 0.63 cm thick acrylic mold, where the 2PP printed master mold is placed tight, as shown in Figure 2 (a). After room temperature curing, the positive mold is peeled off from the master mold with empty channels to be filled with the conductive electrode material. Figures 2 (b) and (c) show the positive mold with DMSO evaporated forming composite substrate maintaining structural integrity and master mold after peeling off with few particles stuck to it, respectively.

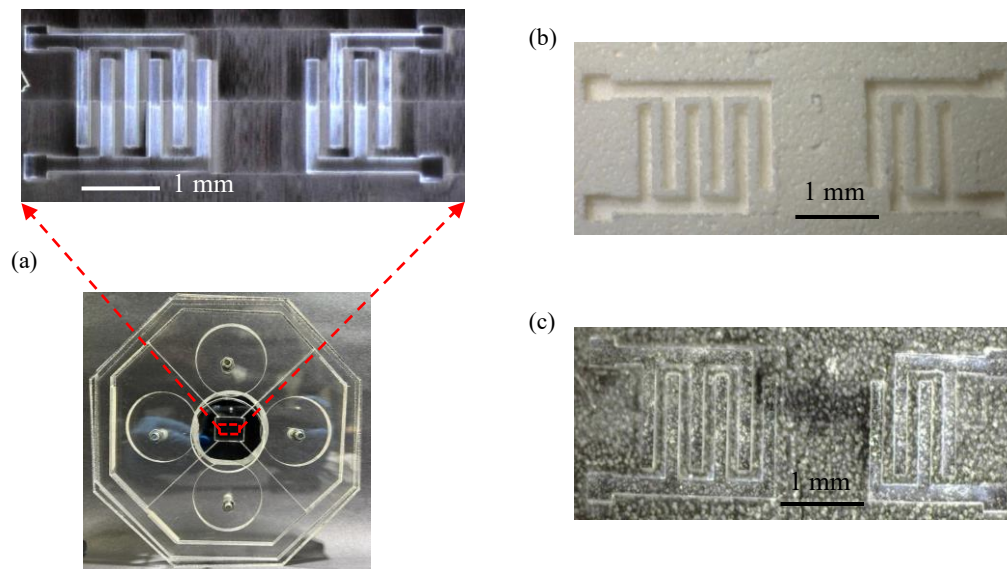


Figure 2. (a) Master mold placed in the acrylic mold where the mixed material is poured in for curing, (b) Piezoelectric positive mold peeled off after curing with electrode channels, and (c) Master mold after peeling

2.3 Surface morphology of the fabricated substrate

To investigate the nanofiller distribution in the polymer matrix, the fabricated substrate is examined using a scanning electron microscope. For better conductivity, samples are sputtered with gold, and images are captured at 10 kV with 4.0

spot size. As shown in Figure 3, pure PVDF-TrFE along with 40 wt. % and 60 wt. % of BT are analyzed. Pure PVDF-TrFE resembles a foamy texture with pores and is overly soft. Composite combination with 40 wt. % exhibits flexibility with less stiffness and pores, making it unsuitable for electrode deposition. In 60 wt. % combination, BT particles have well adhered with less porosity and uniform dispersion, suitable for embedding electrodes with sturdiness. BT particle with an average particle size of 420 nm is observed through particle size distribution analysis based on 382 particles, as shown in Figure 3 (c).

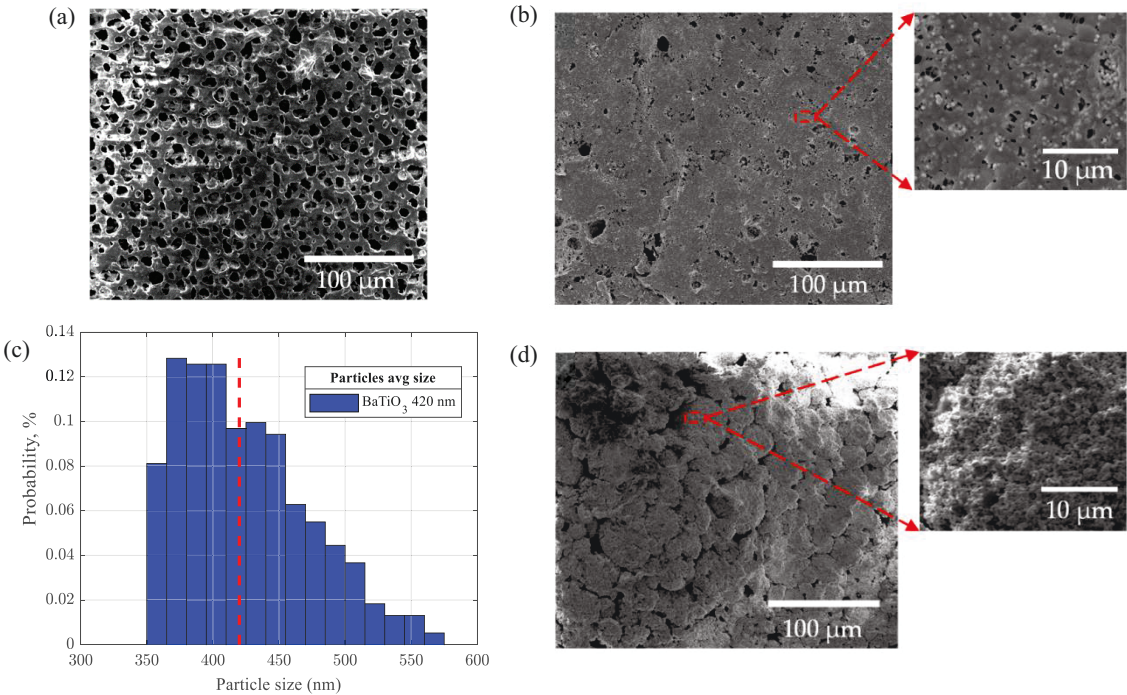


Figure 3. SEM images (a) PVDF-TrFE; (b) PVDF-TrFE with 40% BT; (c) BT Particle distribution and (d) PVDF-TrFE with 60% BT

2.4 Piezoelectric and mechanical property measurement

Piezoelectric properties are important physical attributes in developing an efficient acoustic sensor substrate. Piezoelectric strain coefficient (d_{33}) is measured in the thickness direction using a YE2730A piezometer.

Material	d_{33} (10^{-12} C/N)		F (β)
	Unpolarized	Polarized	
PVDF-TrFE	21.5	23.8	73.1%
PVDF-TrFE/ 40 wt. % BT	28	29.3	75.9 %
PVDF-TrFE/ 60 wt. % BT	33.7	36.5	78.5 %

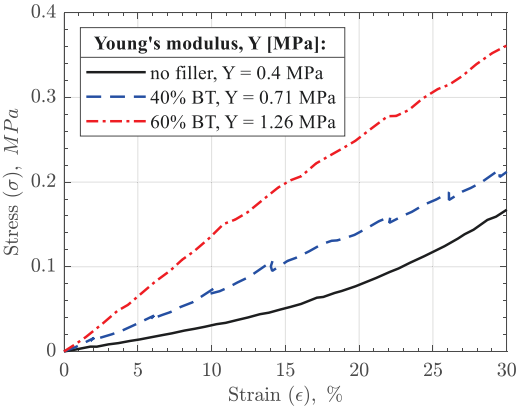


Figure 4. Piezoelectric strain coefficients measured for different piezoelectric composite types and their Young’s modulus

The conversion of the non-polar phase to an active phase is carried out by applying a high voltage of 8 kV through a non-contact poling process, which enhances the piezoelectric property by aligning the dipoles towards the electric field direction. A maximum d_{33} value of 36.5 pC/N is achieved in a composite with 60 wt. % BT, with an 8.5% increase after polarization. A compression test is performed using a universal testing machine AMETEK CS225 (Berwyn, PA, USA) with a 10 kg load cell at a 1 mm/min extension rate. When comparing pure PVDF-TrFE with 40 and 60 wt. % BT combinations, increase in stiffness is observed as the particle loading increased. A maximum Young's modulus of 1.26 MPa is obtained with 60 wt. % BT maintaining stiffness and pliability. Measured piezoelectric strain coefficients, young's modulus, along with crystalline phase information are listed in Figure 4.

2.4 Crystalline phase characterization by FT-IR Spectroscopy

Fourier transform infrared spectroscopy (FT-IR) using an Agilent ATR FTIR is executed to quantitatively analyze the presence of the crystalline phase, which dominates the piezoelectricity of PVDF-TrFE polymer¹⁶. Infrared spectra in a wavenumber range of 750-1550 cm^{-1} are obtained using an Agilent spectrometer. Figure 5 shows absorption peaks at 763 cm^{-1} and 952 cm^{-1} representing non-polar α phase, while peaks at 841 cm^{-1} (CF_2 symmetric stretching), 1172 cm^{-1} and 1280 cm^{-1} (CF_2 symmetric stretching), originate due to β phase presence. Additionally, the peak at 1401 cm^{-1} is due to CH_2 wagging vibration. The peaks at 880 cm^{-1} and 1172 cm^{-1} correspond to the a-axis, 841 cm^{-1} and 1280 cm^{-1} peaks indicate the polar b-axis, and 1401 cm^{-1} peak is associated with the c-axis of the polymer chain¹⁷⁻¹⁹.

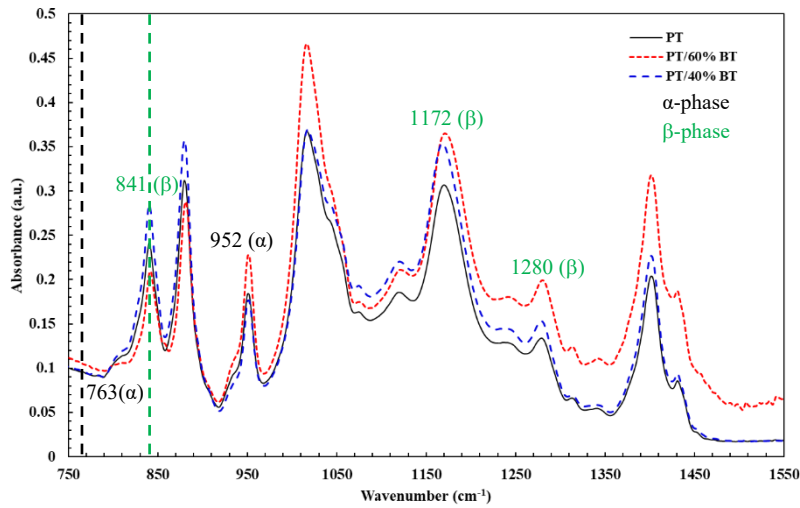


Figure 5. FT-IR absorbance spectra for PVDF-TrFE (PT) polymer with 40% and 60% BT

Based on the Beer-Lambert law, the fraction of active β phase in different composite types is calculated using equation (1),

$$F_{\beta} = \frac{A_{\beta}}{\left(\frac{k_{\alpha}}{k_{\beta}}\right) A_{\alpha} + A_{\beta}} \quad (1)$$

where A_{α} and A_{β} are the absorbance peak intensities at 763 cm^{-1} and 841 cm^{-1} , respectively and k_{α} and k_{β} are $7.7 \times 10^4 \text{ cm}^2 \text{ mol}^{-1}$ and $6.1 \times 10^4 \text{ cm}^2 \text{ mol}^{-1}$ representing the absorption coefficient at the corresponding wavenumber. As listed in Table 1, it is evident that adding nanofillers increases the β phase with d_{33} enhancement and a maximum polar phase of 78.5 % is achieved with 60 wt.% BT fillers.

3. IDT ELECTRODE DEPOSITION

A screen-printing technique is used to deposit the conductive material (filling the empty channel in the positive mold with electrodes). A stencil with an IDT pattern is designed and developed using a 2PP printer, which acts as a mask where the conductive material is transferred onto the positive mold, except in areas made impermeable to the ink by a blocking mesh. The printing parameters used for developing a stencil are the same as the master mold printing. Figures 6 (a) and (b) show the CAD model of a stencil with IDT pattern and 2PP printed stencil. The electrodes are made of conductive poly(3,4-ethylenedioxythiophene)-poly(styrenesulfonate) (PEDOT:PSS) 5% screen printable ink (Sigma-Aldrich, St. Louis, MO, USA). IDT pattern made of conductive PEDOT:PSS ink is screen printed without discontinuity with a minor spread of ink, due to the foamy nature of PVDF-TrFE, and is well bonded to the base substrate, as shown in Figure 6 (c). Figure 6 (d) shows the stencil condition after screen printing and cleaned using water, which can be reused.

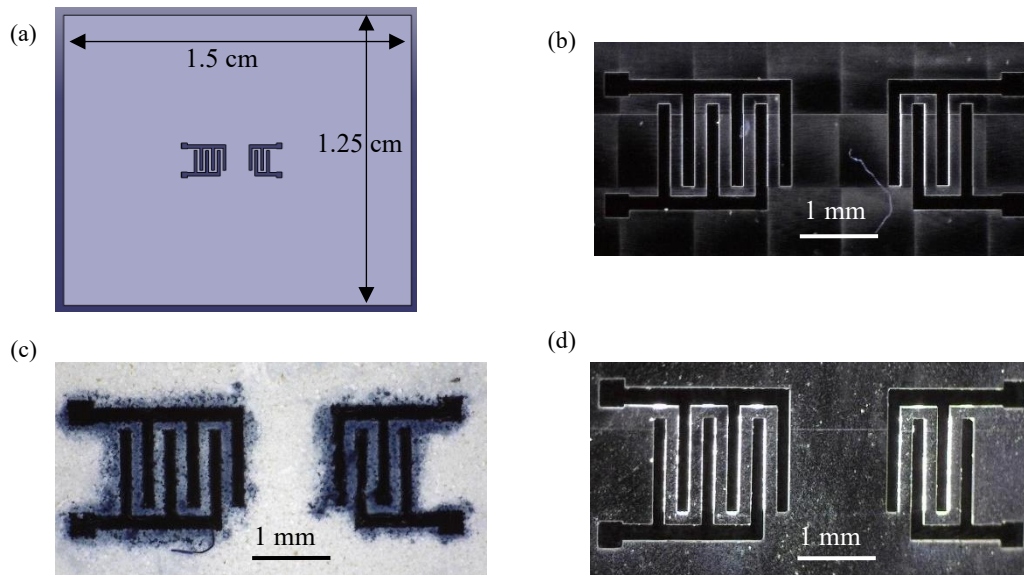


Figure 6. (a) CAD model of stencil with empty IDT pattern; (b) 2PP printed stencil; (c) electrode channel filled with conductive material; and (d) stencil after electrode filling

4. STRAIN DETECTION TESTING

Frequency response analysis is carried out using a spectrum vector analyzer (Siglent SVA 1032X) to evaluate the strain detection capability of the fabricated piezoelectric sensor with embedded electrodes. The network analyzer GGB probes (ECP 18-GSG-1250-DP) are connected to the IDT terminals of the sensor attached to a flat and 30° curved steel surface (host structure), as shown in Figure 7 (c). The probes are calibrated using a CS-10 calibration substrate, and sensor response is measured in the frequency range from 80 MHz to 130 MHz providing information of mechanical strains that occurred in the host structure. A 10 dBm RF signal is provided as an input to the sensor with a reference impedance of 50 Ω to analyze the scattering parameter (S_{21}). The frequency response depends on the IDTs pattern, electromagnetics of the material, and the velocity of the acoustic wave generated. The S_{21} response of the developed sensor measured at a flat and angled condition is represented in Figures 7 (a) and (b). When a strain occurs in the host structure, there is a perceptible frequency shift and peak intensity relational to the change in wave characteristics, which validates the strain detection capability of the developed piezoelectric sensor. A harmonic frequency shift is detected from 103 MHz to 109 MHz for the PVDF-TrFE/BT sensor with higher piezoelectric and mechanical properties. Some parasitic effects are noticed due to electromagnetic coupling in probe setup and impedance mismatch, which leads to missing fundamental peak detection.

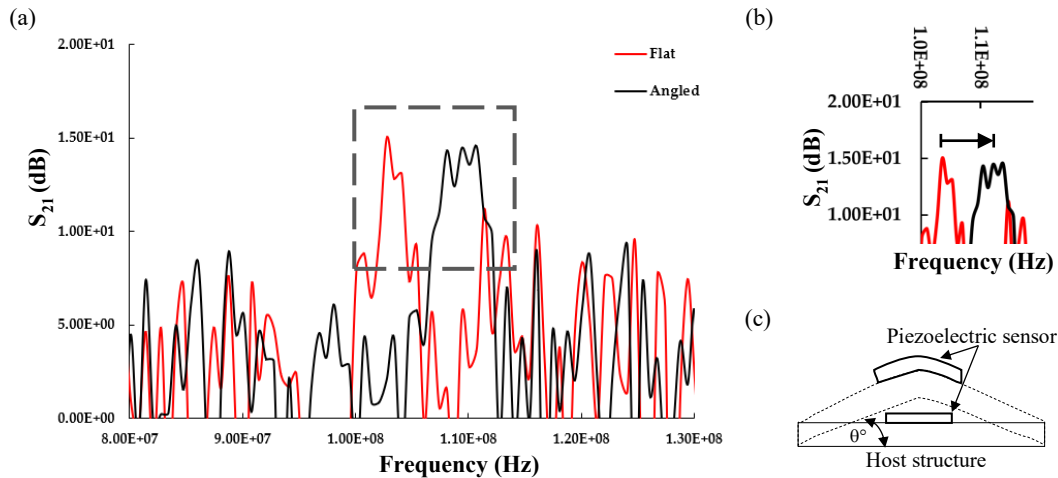


Figure 7. (a) Frequency response of piezoelectric sensor measured in both flat and bent (30°) condition; (b) zoomed-in response shows the frequency shift details and (c) strain validation setup with a sensor attached to host structure at an angle θ°

5. CONCLUSION

In summary, a piezoelectric acoustic sensor based on PVDF-TrFE and BT nanofiller with embedded electrodes is successfully developed through a novel reverse replication process using a 2PP printed master mold and stencil. The effect of adding nanofiller to the polymer matrix is studied through surface morphology, chemical characterization, mechanical and piezoelectric property measurements. PVDF-TrFE with 60 wt.% BT yielded the maximum piezoelectric strain coefficient (d_{33}) of 36.5 pC/N with 78.5% active crystalline phase. Mechanical strains are detected using the frequency shift information through RF probing setup. In the future, experiments will be performed with optimized and decreased electrode dimensions, maintaining the IDT pattern for efficient wave generation and investigation of frequency measurement to avoid the influence of secondary effects.

ACKNOWLEDGMENT

This material is based upon work supported in part by the National Science Foundation under Grant No. 2018853.

REFERENCES

- [1] Ji, Z., and Zhang, M., "Highly sensitive and stretchable piezoelectric strain sensor enabled wearable devices for real-time monitoring of respiratory and heartbeat simultaneously," *Nanotechnology and Precision Engineering*, 5(1), 013002 (2022).
- [2] Thakur, A., "Structural Health Monitoring Through the Application of Piezoelectric Sensors—State of the Art Review," *Advances in Construction Materials and Sustainable Environment*, 657-673 (2022).
- [3] Gimenes, R., Zaghete, M. A., Bertolini, M. *et al.*, "Composites PVDF-TrFE/BT used as bioactive membranes for enhancing bone regeneration," *Smart Structures and Materials 2004: Electroactive Polymer Actuators and Devices (EAPAD)*. 5385, 539-547.
- [4] Srinivasaraghavan Govindarajan, R., Rojas-Nastrucci, E., and Kim, D., "Strain sensing using flexible surface acoustic wave sensor," *Sensors and Smart Structures Technologies for Civil, Mechanical, and Aerospace Systems 2020*. 11379, 1137912.
- [5] Valiyaneerilakkal, U., and Varghese, S., "Poly (vinylidene fluoride-trifluoroethylene)/barium titanate nanocomposite for ferroelectric nonvolatile memory devices," *Aip Advances*, 3(4), 042131 (2013).
- [6] Siponkoski, T., Nelo, M., Jantunen, H. *et al.*, "A printable P (VDF-TrFE)-PZT Composite with Very High Piezoelectric Coefficient," *Applied Materials Today*, 20, 100696 (2020).

- [7] Belovickis, J., Ivanov, M., Svirskas, Š. *et al.*, "Dielectric, Ferroelectric, and Piezoelectric Investigation of Polymer-Based P (VDF-TrFE) Composites," *Physica status solidi (b)*, 255(3), 1700196 (2018).
- [8] Shi, K., Chai, B., Zou, H. *et al.*, "Interface induced performance enhancement in flexible BaTiO₃/PVDF-TrFE based piezoelectric nanogenerators," *Nano Energy*, 80, 105515 (2021).
- [9] Vacche, S. D., Oliveira, F., Leterrier, Y. *et al.*, "The effect of processing conditions on the morphology, thermomechanical, dielectric, and piezoelectric properties of P (VDF-TrFE)/BaTiO₃ composites," *Journal of Materials Science*, 47(11), 4763-4774 (2012).
- [10] Zhang, Q., Han, T., Tang, G. *et al.*, "SAW characteristics of AlN/SiO₂/3C-SiC layered structure with embedded electrodes," *IEEE Transactions on Ultrasonics, Ferroelectrics, and Frequency Control*, 63(10), 1608-1612 (2016).
- [11] Srinivasaraghavan Govindarajan, R., Rojas-Nastrucci, E., and Kim, D., "Surface Acoustic Wave-Based Flexible Piezocomposite Strain Sensor," *Crystals*, 11(12), 1576 (2021).
- [12] Busche, J. F., Starke, G., Knickmeier, S. *et al.*, "Controllable dry adhesion based on two-photon polymerization and replication molding for space debris removal," *Micro and Nano Engineering*, 7, 100052 (2020).
- [13] Pérez, M., Carou, D., Rubio, E. M. *et al.*, "Current advances in additive manufacturing," *Procedia Cirp*, 88, 439-444 (2020).
- [14] Srinivasaraghavan Govindarajan, R., Xu, X., Sikulskyi, S. *et al.*, "Additive manufacturing of flexible nanocomposite SAW sensor for strain detection," *Sensors and Smart Structures Technologies for Civil, Mechanical, and Aerospace Systems 2021*. 11591, 115910F.
- [15] Bunea, A.-I., del Castillo Iniesta, N., Droumpali, A. *et al.*, "Micro 3D Printing by Two-Photon Polymerization: Configurations and Parameters for the Nanoscribe System," *Micro*. 1, 164-180.
- [16] Legrand, J., "Structure and ferroelectric properties of P (VDF-TrFE) copolymers," *Ferroelectrics*, 91(1), 303-317 (1989).
- [17] Jia, N., He, Q., Sun, J. *et al.*, "Crystallization behavior and electroactive properties of PVDF, P (VDF-TrFE) and their blend films," *Polymer Testing*, 57, 302-306 (2017).
- [18] Yuan, X., Gao, X., Shen, X. *et al.*, "A 3D-printed, alternatively tilt-polarized PVDF-TrFE polymer with enhanced piezoelectric effect for self-powered sensor application," *Nano Energy*, 85, 105985 (2021).
- [19] Mao, D., Gnade, B. E., and Quevedo-Lopez, M. A., "Ferroelectric properties and polarization switching kinetic of poly (vinylidene fluoride-trifluoroethylene) copolymer," *Ferroelectrics-Physical Effects*, 78-100 (2011).